Electronic Supplementary Material (ESI) for Lab on a Chip

Custom tailoring multiple droplets one-by-one

Jan Guzowski, Sławomir Jakieła, Piotr M. Korczyk, and Piotr Garstecki

Supporting Information

I. Derivation of the protocol V(n) for the generation of an ensemble of droplets with a given volume distribution p(V).

Let us assume that V(n) is a monotonic function describing the volume of the n'th generated droplet. Then the number Δn of droplets of the volume between V and V+ΔV equals $\Delta n(V,V+\Delta V)\approx\Delta V/(dV/dn)$. Dividing by the total number n_{tot} of generated droplets and taking the limit $\Delta V\to 0$ we obtain

$$p(V)=1/(n_{tot}\cdot dV/dn), \tag{1}$$

where $p(V):=\lim_{\Delta V\to 0}\Delta n/(\Delta V n_{tot})$ is the density distribution of the generated volume. Integrating Eq. (1) we obtain $P(V)=n/n_{tot}$, where $P(V)=\int dVp(V)$ is the cumulative distribution, so that

$$V(n)=P^{-1}(n/n_{tot}). \tag{2}$$

From this we also see that, as P(V) is from definition monotonic, V(n) is always well defined. In experiment we generated the log-normal distribution $p(V^*)=\exp[-(\ln V^*-\mu)^2/(2\sigma^2)]/(V^*\sigma\sqrt{2\pi})$ with μ=-1.4, σ=0.7 and $V^*=(V-V_{min})/(V_{max}-V_{min})$, where V_{min}/W^3=1.8 and V_{max}/W^3=13.9 were chosen as the minimal and maximal generated volume, respectively. (We note that with our technique V_{min} is always limited from below by the dead volume of the junction $V_{dead}/W^3\cong 1$.) Accordingly, the input protocol (plotted as the solid line in Fig. 2a) was calculated as $V(n)=V_{min}+(V_{max}-V_{min})P^{-1}(n/n_{tot})$, where P^{-1} was the inverse of the cumulative distribution P(V*). The corresponding density distribution was analogically calculated as $p(V)=p(V^*)W^3/(V_{max}-V_{min})$. In order to compare with the experimentally measured values $\Delta n(V,V+\Delta V)$ we approximated $\Delta n(V,V+\Delta V)\approx p(V)n_{tot}\Delta V$ (plotted as the solid line in Fig. 2b)

II. Derivation of the volume distribution p(V) corresponding to the given profile of release M(t).

Release of the encapsulated substance from an ensemble of capsules characterized by the distribution p(V) can be written as

$$M(t)=\int dVp(V)m(V,t), \tag{3}$$

where m(V,t) is the amount of released substance (say, in percent, such that m and M are both non-dimensional) from a single shell of volume V after time t. We note that m(V,t) is

only well defined if we assume a uniform thickness of the shell, i.e., a perfectly central core. For example, centering of the core inside the shell seems to happen spontaneously in the case of a thin and relatively viscous shell [1]. Otherwise, one could consider using an external electric field, which then would require a proper choice of the ratios of the dielectric constants of the working fluids [2]. Assuming that the core is centered, the shell is impermeable to the encapsulant and soluble in the outer (e.g. bodily) liquid-such that its thickness decreases with time-the release would occur as a delayed burst (at the moment when the thickness of the shell becomes zero).[21] Approximating $m(V,t)=\Theta(t-t_0(V))$, where $t_0(V)$ is the time after which the shell of volume V bursts (it could be calculated [3] or measured [4]), with Θ being the Heaviside step-function, and taking the time derivative of both sides in Eq. (3) we obtain (using notation $f'(x):=df/dx$)

$$M'(t) = \int dV p(V)\delta(V-t_0^{-1}(t))/|t'_0(V)| = p(t_0^{-1}(t))/|t'_0(t_0^{-1}(t))|. \quad (4)$$

Taking $t=t_0(V)$ we finally get $M'(t_0(V)) = p(V)/|t'_0(V)|$, so that

$$p(V)=|t'_0(V)|\cdot M'(t_0(V)). \quad (5)$$

In the case of sufficiently thin shells one can use the approximation $t_0(V)=CV+D$, with constants $C>0$ and D, and then $p(V)/C=M'(CV+D)$. Accordingly, for example, a delayed, extended release characterized by $M'(t)$ with a peak at a certain positive $t=t_{release}$ and a long tail for $t>t_{release}$, would correspond to p(V) with the same characteristics, i.e., with a peak at $V_0=(t_{release}-D)/C$ and a long tail for $V>V_0$. In our experiment, we used a log-normal distribution (Fig. 2) as an analytically tractable example.

III. Experimental determination of the critical volume ratios k_1 and k_2 in the case of N=4 identical cores.

We generated shells containing N=4 cores for various total volumes V_{shell} of the shell and the cumulated volume V_{core} of the cores by changing the supplying pressures while keeping the opening times of the valves constant. We estimated the volumes by measuring the lengths of the droplets in the inlet channel. Then, we observed the relaxation in the wider channel and classified the structures according to their mode of generation (spiral, zig-zag or linear) and shape (square, rhombic or linear). The results, presented in Fig. S1 are consistent with our expectation that the final structures depend mainly on the volume fraction $k=V_{core}/(V_{core}+V_{shell})$ rather than separately on each volume. We calculated the critical values k_1 and k_2 of the volume fraction corresponding to square-to-rhombic and rhombic-to-linear transitions, respectively, of the shape of the final structure, by fitting lines passing through the origin to the points separating the regions (marked on Fig. S1 with red contour). The resulting values were $k_1=0.66\pm0.03$ and $k_2=0.80\pm0.03$.

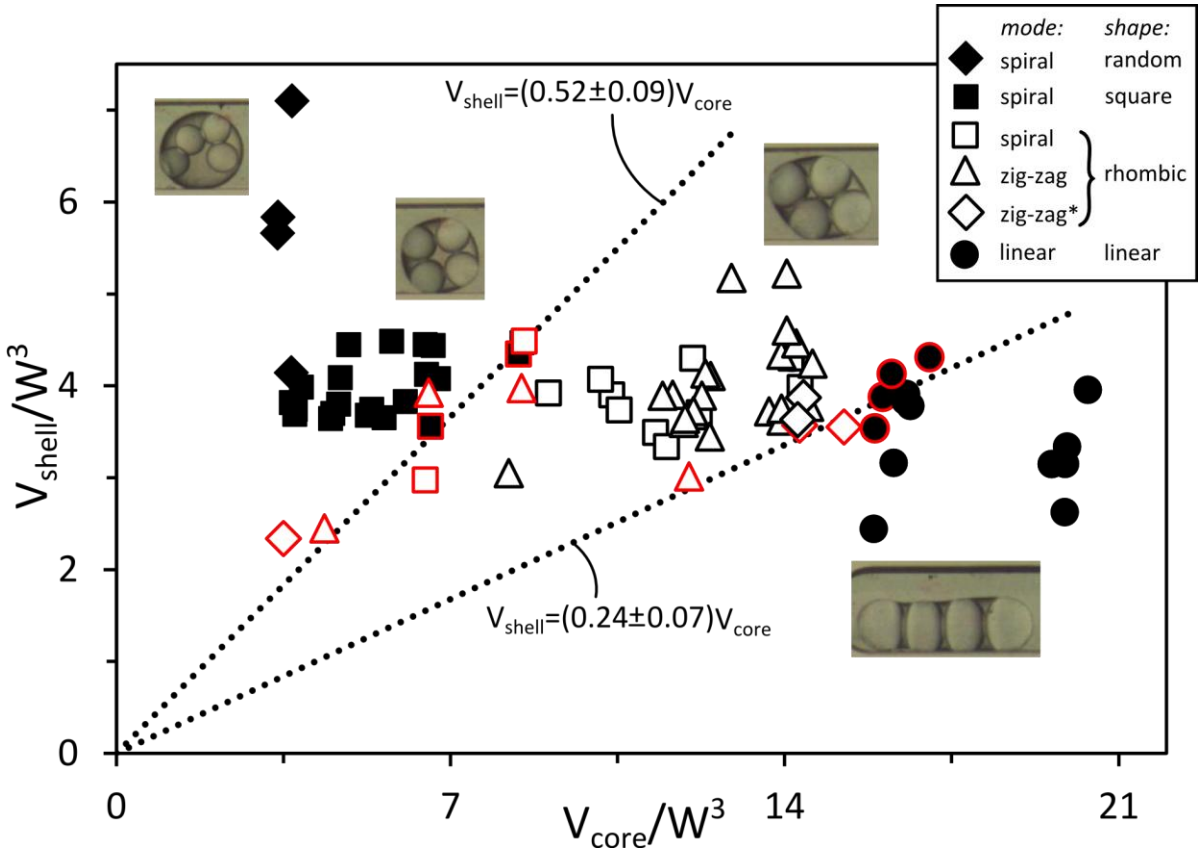

Fig. S1. Mode of generation and the shape of the final structure in the case of N=4 identical cores depending on the volumes V_{shell} and V_{core} of the shell and the cores. The dotted lines are the linear fits to the points marked with red contour. The critical volume fractions calculated from the linear fits were $k_1=0.66\pm0.03$ and $k_2=0.80\pm0.03$. The shapes denoted as random correspond to the situation in which the cores can move freely inside the shell. The encapsulated phase was pure water (without dye), while the composition of the remaining phases was as described in the main text of the paper.

IV. Metastable states in the case of one small and three large cores.

In Fig . S2 we show three different metastable structures observed in the case N=4 with one small and three large cores. The only structure which we could systematically reproduce was structure vii, which occurred independently of the particular sequence (note that on the snapshot in Fig. S2 the structures are not squeezed by the side-walls). The other metastable states viii and ix could be achieved by stopping the flow after generation of each consecutive core. Also we observed that the planar structure viii was metastable with respect to tetrahedral structure ix, i.e., it frequently happened that the former spontaneously folded into the latter after a few seconds, but the opposite never happened. In contrast structures vii was stable for the typical observation time of up to appr. 1 min.

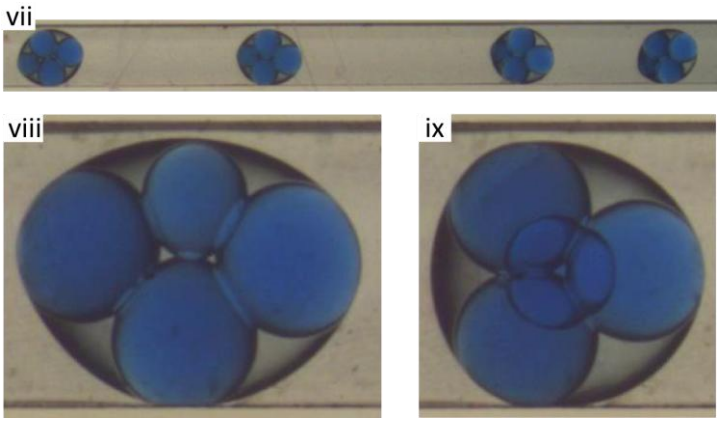

Fig. S2. The reproducible structures (vii), not confined by the side-walls of the outlet channel and close-up views of two other metastable structures (viii, ix) as obtained in the case of 1 small and 3 large cores. The structure ix was a tetrahedron in which the small core can be seen from behind the large ones.

V. Generation of sequences of different multiple droplets.

We generated a sequence of multiple droplets (Fig. S3 a) each containing a different number N of identical cores in the range N=1,…,7. Note the three dimensional structures emerging for N≥5. The structures were reproducible but in general dependent on the size of the cores and their volume fraction in the shell. We leave a detailed study of this dependence for later work. We also generated a series of droplets each containing a different sequence of large and small cores for N≤3 (Fig. S3 b).

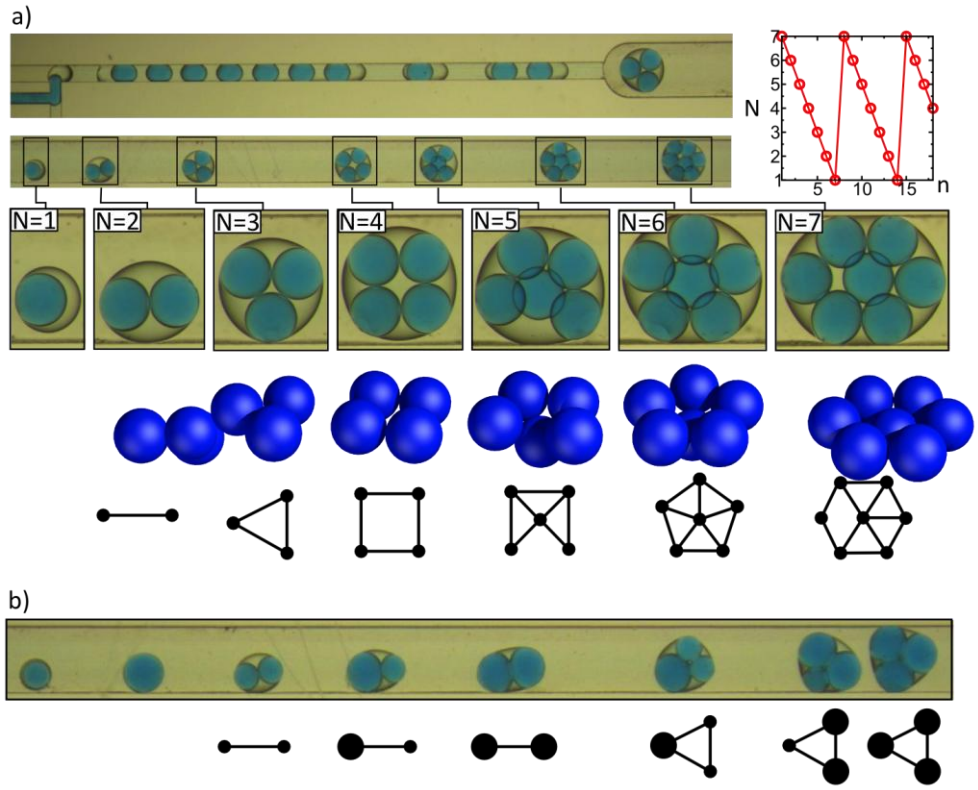

Fig. S3. a) A sequence of shells (on the plot n indexes the shells) containing periodically decreasing number N of identical cores from N=7 to N=1. Below: visualization of the 3D arrangement of cores and diagrams of their connectivity. b) A sequence of shells containing all possible combinations of small and large cores for N≤3.

VI. The device for generation of multiple droplets with two different kinds of cores.

In Fig. S4 we show a scheme of the device equipped with an additional inlet supplying the second encapsulated phase. The geometry of the junction was designed such that it prevented contact between the encapsulated phases at the junction. The important elements of the design were the lengths L and L_2 and the widths W and W_2 of the channels. In order to prevent generation of the droplets in the direction upstream the junctions the sum of hydrodynamic resistances of both branches L_2 should be larger than the resistance of the branch L. As the resistance of the channels grows as $\sim L/W^4$, the above requirement leads to the condition $2L_2/L > (W_2/W)^2$. In designing the device we took into consideration the fact that generation of droplets at one of the junctions, say of phase A, should not lead to significant relative increase of the resistance of the junction, because this would lead to the decrease of the flow of phase B at this junction (and its proportional increase at the opposite junction) which in turn would prevent generation of droplets due to not sufficiently strong shear. Accordingly, the length of the branch L_2 must be as large as possible. In our study we used $L_2/W_2=10$.

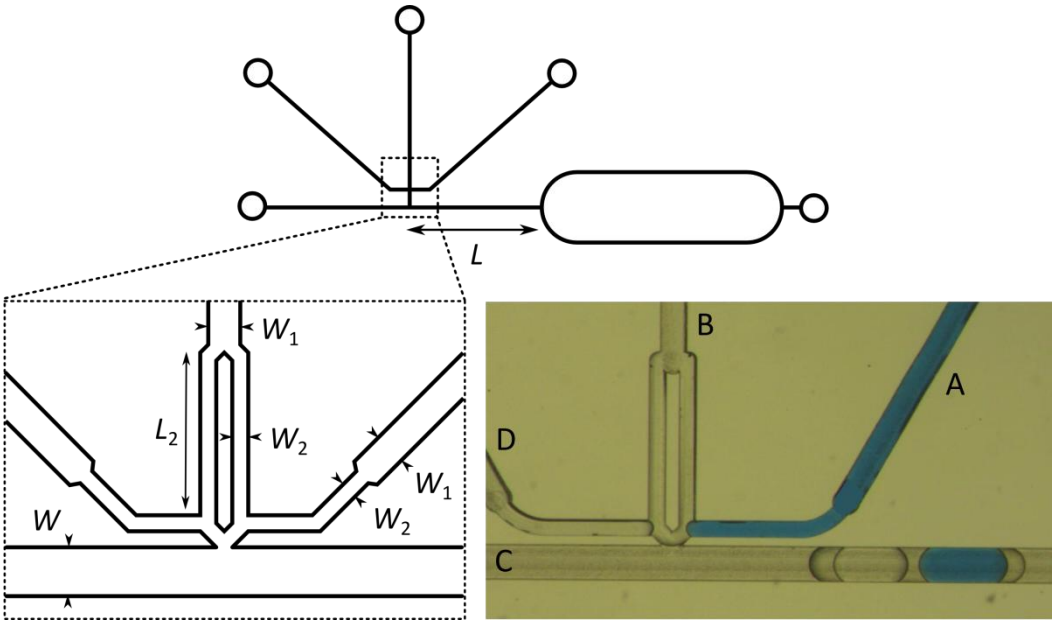

Fig. S4. A scheme of the triple T-junction for simultaneous encapsulation of species A (water with 0.1% w/w Methylene Blue dye) and D (pure water). The widths of the channels are W=300 μm, W_1=200 μm, W_2=100 μm and the lengths L=10 mm and L_2=1 mm.

VII. Additional protocols for generation of ensembles droplets with a single core.

We have generated sequences of droplets with i) constant volume of the core and the volume of the shell (and the total volume) changing linearly or as a sine function of n (Figs. S5 a and c), and ii) constant total volume and the volume of the core and the shell changing

linearly or as a sine function of n (Fig. S5 b and d). In Fig. S5 the sizes of the droplets are expressed directly in terms of their lengths in the narrow channel.

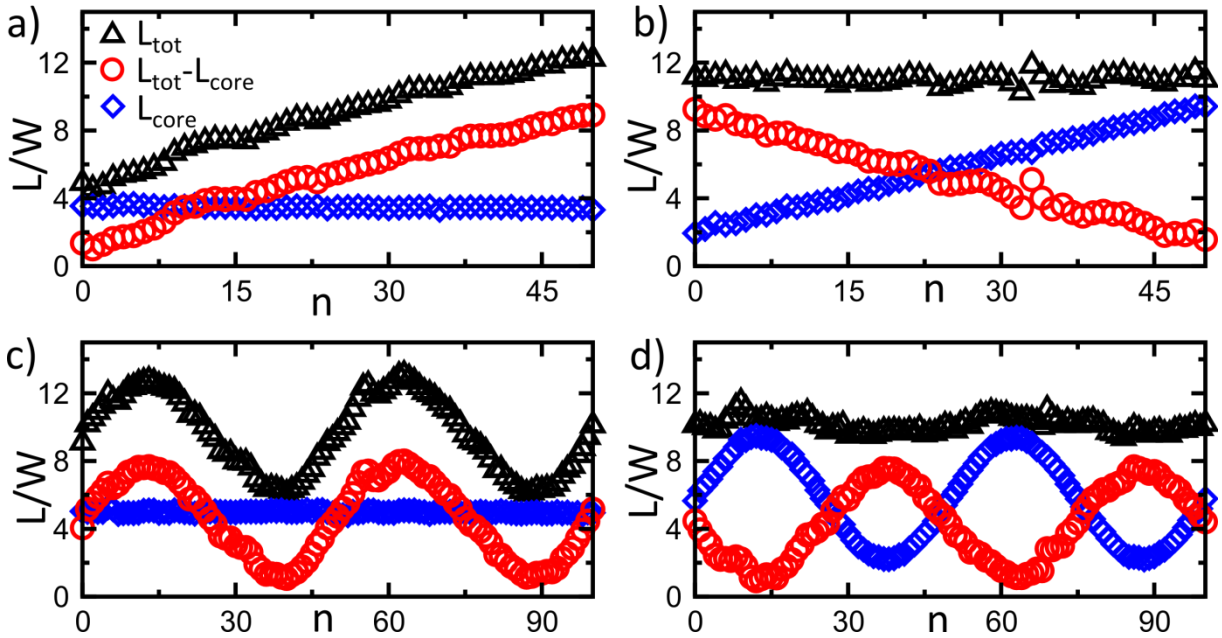

Fig. S5: Sequences of lengths (proportional to volumes) of the droplets generated according to various protocols L(n). a) L_{core}=const, L_{tot}~n, b) L_{core}~n, L_{tot}=const, c) L_{core}=const, L_{tot}~sin(4πn/100), d) L_{core}~sin(4πn/100), L_{tot}=const.

VIII. Movies

The files movie01 and movie02 show periodic generation of a sequence of multiple droplets containing a decreasing number of identical cores from N=7 to N=1. Note that the connectivity of the cores, also analyzed in Fig. S3, is reproducible. The file movie03 shows generation of a sequence of multiple droplets encoding the phrase 'online control' according to the Morse alphabet. Each droplet encodes a single letter with small and large cores corresponding to dots and dashes, respectively.

References:

[1] Y. Hennequin, N. Pannacci, C. P. de Torres, G. Tetradis-Meris, S. Chapuliot, E. Bouchaud and P. Tabeling, *Langmuir*, 2009, **25**, 7857-7861.

[2] Z. Bei, T. B. Jones, D. R. Harding, *Soft Matter*, 2010, **6**, 2312-2320.

[3] N. Shankar, T. J. Wiltshire and R. S. Subramanian, *Chemical Engineering Communications*, 1984, **27**, 263-281.

[4] S. Suzuki, T. A. Asoh and A. Kikuchi, *Journal of Biomedical Materials Research Part A*, 2013, **101A**, 1345-1352.